HADES Overview

Recent results from measurements probing the high μ_B / high net-baryon density region of the QCD phase diagram

Simon Spies[1,*] *et al.* HADES Collaboration

[1]Goethe-University Frankfurt, Germany

Abstract. In this contribution we present results from Au+Au collisions at $\sqrt{s_{NN}}$ = 2.42 GeV as well as Ag+Ag collisions at $\sqrt{s_{NN}}$ = 2.42 and 2.55 GeV measured by HADES. We focus on three different observables: electromagnetic probes, collective and bulk-matter phenomena and strangeness production which are discussed in the following.

1 Introduction

The HADES detector located at the GSI Helmholtz Center for Heavy-Ion Research in Darmstadt, Germany is a versatile fixed-target collision experiment. It is operated with few GeV ion beams provided by the SIS18 synchrotron. The state of the systems created in such collisions at freeze-out is characterized by the highest baryo-chemical potentials probed by currently running experiments and intermediate temperatures. Similar properties of matter are expected to be formed in merging neutron stars [1–3] which is why heavy-ion collisions at low energies provide a unique opportunity to study the microscopic and ultimately also macroscopic properties of such matter. Furthermore, HADES can also be operated with proton or secondary pion beams to study for example the properties of hadronic resonances and provide reference measurements for heavy-ion collisions.

In heavy-ion collisions at low energies, the nucleons are essentially stopped in the collision zone resulting in a strong domination of (net-)baryons over mesons in the created system. While ab initio lattice-QCD calculations [4] successfully describe static baryon-anti-baryon symmetric matter and can thereby be applied to heavy-ion collisions at high collision energies, they are challenged at systems with strong baryon-anti-baryon asymmetry by the fermion determinant sign problem. Therefore, the description of such systems requires effective approaches to QCD combined with microscopic transport models [5–7] to mimic the collision dynamics.

The detector setup of HADES is schematically depicted in an expanded view in figure 1. Starting from the segmented 15-fold gold/silver target, particles traverse a Ring-Imaging CHerenkov (RICH) detector for e^+/e^- identification, two low-mass Mini Drift Chamber (MDC) tracking stations, a toroidal magnetic field, followed by two further MDC tracking stations and depending on the polar angle either a Resistive Plate Chamber (RPC) or a Time Of Flight (TOF) scintillation detector for the time of flight measurement. The setup is completed by an Electromagnetic CALorimeter (ECAL) for photon detection, a Forward Wall

*e-mail: s.spies@gsi.de

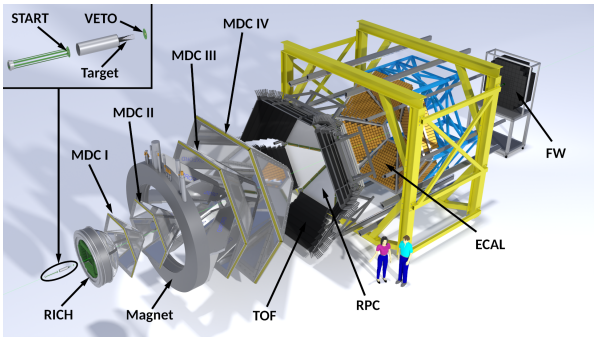

Figure 1. Schematic expanded view of the HADES detector setup. Coming from the lower left, the beam-ions traverse the START detector, the target and in case of no interaction the VETO detector. The emitted particles are measured by the RICH, four MDC planes, the RPC or TOF and the ECAL detector. Finally, the FW detector measures spectator nucleons.

(FW) hodoscope for measurement of the event plane and a diamond reaction time and trigger detector (START) located in front of the target. Besides the RICH, the FW, the START and the VETO detector, all detectors are split into six independent sectors covering almost the entire azimuthal angle. More details on the HADES experiment are given in [8].

2 Electromagnetic Probes

The measurement of electromagnetic radiation emitted from the fireball using di-leptons is an ideal tool to probe the properties of the hot and dense phase of the reaction as leptons traverse the nuclear matter without distortion from the strong interaction. The integrated spectrum of di-leptons emitted from heavy-ion collisions contains contributions from several sources which can be attributed to three steps of the evolution of the fireball:

The initial state contribution results from early p+p, p+n and n+n collisions and can be estimated via reference measurements in small collision systems for example measured by the DLS experiment [9]. HADES has previously revealed that isospin effects cause strong differences between the emission of di-leptons from p+p / n+n and p+n collisions [10]. The second contribution is attributed to thermal radiation emitted by the fireball. As such, its spectrum allows for a direct measurement of the temperature of the emitting system. Furthermore, HADES demonstrated that the Vector-Meson-Dominance model, assuming thermal radiation to be emitted from nuclear systems via intermediate vector mesons, provides a good description of the measured spectra [1, 11]. The final contribution to the di-lepton spectrum results from decays of hadrons emitted from the fireball. At HADES energies, it contains contributions from dalitz decays of predominantly π^0, η and ω mesons as well as di-lepton decays from ω and ϕ mesons. The latter contribution allows us to deduce information on the modification of mesons in dense nuclear matter via peak-position and -width measurements of the corresponding signals.

Figure 2 shows in the left the invariant mass spectrum of di-leptons after subtraction of the combinatorial background measured in the 0-40% most central Au+Au collisions at $\sqrt{s_{NN}}$ = 2.42 GeV. The black and red data points correspond to two different analysis techniques which yield compatible results and the blue data points correspond to the NN reference measurement. The cyan curves show different contributions to the hadronic cocktail. Depicted are the dalitz decays of π^0, η and ω mesons as well as di-lepton decays of ω and ϕ mesons. The contribution of the di-lepton decay of ρ mesons is not included since, due to its short lifetime, ρ mesons decay inside the dense medium where their mass distribution is modified, which is seen in the spectrum as the excess radiation above the π^0 mass. The right part of figure 2 shows the invariant mass distribution of this excess radiation extracted by subtracting the NN reference and hadronic cocktail contributions. The red curve corresponds to a Planck function and shows that the spectrum can be described as thermal radiation from a source

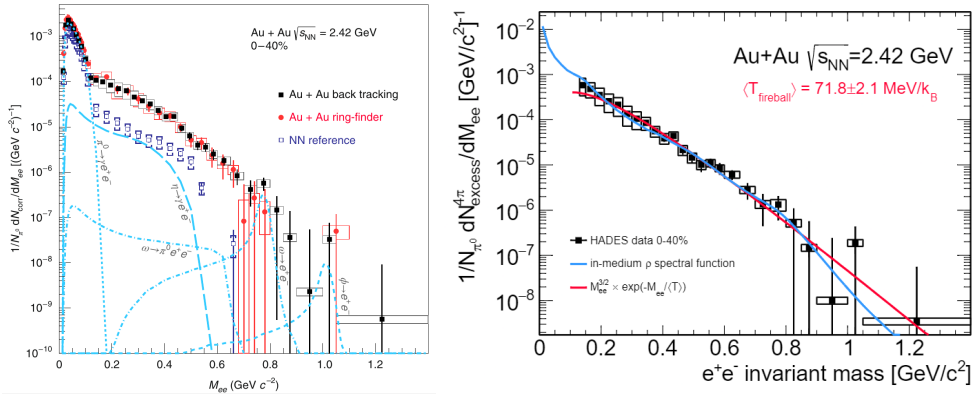

Figure 2. Invariant mass spectra of di-leptons emitted from Au+Au collisions at $\sqrt{s_{NN}}$ = 2.42 GeV. The left plot shows the full spectrum obtained via two different reconstruction techniques after background subtraction as well as the NN reference spectrum and the hadronic cocktail contributions. The right plot shows the spectrum of the excess radiation obtained by subtracting the NN reference and the hadronic cocktail contribution from the full spectrum [1].

with an average temperature of 71.8 ± 2.1 MeV/k_B. This temperature can be interpreted as the average temperature of the fireball during its evolution. The blue curve corresponds to a prediction of the thermal emission obtained by applying calculations based on the vector-meson-dominance model [12–14] onto coarse-grained UrQMD transport model predictions and shows a perfect description of the measured spectrum. These observations support that the vector-meson-dominance model properly describes the coupling of ρ mesons to baryonic matter as previously indicated by HADES measurements in pion-induced reactions [11].

3 Collective Flow Phenomena and Two-Particle Correlations

Investigating the correlations between the particles emitted from the fireball allows us to study the properties of the microscopic interactions as well as their implications on the macroscopic properties of the dense matter, for example the equation of state. On a microscopic level, these studies can be performed using the femtoscopy technique to determine the correlation function of two species of particles. It consists of a source function contribution describing the state in which the particles are emitted from the source and an interaction contribution describing how the interactions between the particles alter their relative kinematics. To extract the latter from the measured correlation function, the contribution from the source function has to be subtracted using fits [15, 16]. On a more macroscopic level, the azimuthal emission pattern of particles with respect to the reaction plane is studied [17]. By applying the method of Fourier decomposition to the obtained distributions, the so-called flow coefficients are extracted. Several theories predict in particular the higher order coefficients to be sensitive to the equation of state of the emitting system.

Thanks to the high statistics recorded during the beamtimes of HADES in combination with the large acceptance and the dominance of baryons in the collision system, HADES can measure the flow of protons and light nuclei with unprecedented precision up to the sixth harmonic [18]. Furthermore, flow coefficients are studied multi-differentially as a function of transverse momentum, rapidity and centrality [19]. During this Quark Matter conference, HADES for the first time presented its ability to extract the flow coefficients up to second

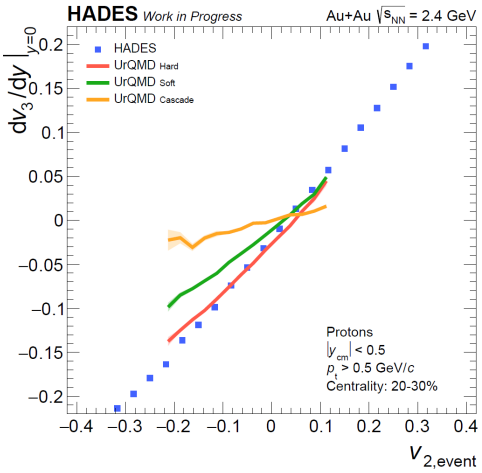

Figure 3. Slope of the triangular flow of protons at mid-rapidity as a function of their elliptic flow calculated event-by-event. The data points correspond to the 20-30% most central Au+Au collisions at $\sqrt{s_{NN}}$ = 2.42 GeV and the curves to predictions of the UrQMD transport model with different equations of state.

order on an event-by-event basis allowing to study the correlations of multiple harmonics with each other. This is highly relevant as several models predict these correlations to be particularly sensitive to the nuclear equation of state.

Figure 3 shows the slope of the triangular flow of protons at mid-rapidity as a function of their elliptic flow calculated event-by-event in the 20-30% most central Au+Au collisions at $\sqrt{s_{NN}}$ = 2.42 GeV. The three curves correspond to predictions from the UrQMD transport model [6, 7] in cascade mode (no nuclear potentials), with a soft and a hard equation of state. At this stage of the investigations, the data favor a hard equation of state which is in agreement with studies of heavy neutron stars whose stability can only be explained by hard nuclear equations of state.

4 Strange Hadrons

At SIS18 collision energies hadrons with strangeness content are produced close to or even blow their energetic threshold in isolated N-N collisions. Thus, their production is strongly correlated to potential medium effects.

In particular, the Λ hyperons and K^0_S mesons can be analyzed in great detail as their off-vertex-decay-topologies, resulting from their large mean lifetimes, allow for a strong suppression of the combinatorial background and therefore the extraction of signals with high significance. At HADES the suppression of the combinatorial background is further enhanced by applying an artificial neural network trained on simulated signals and combinatorial background [20, 21]. Using the same method, also the light hypernuclei, ${}^{3}_{\Lambda}H$ and ${}^{4}_{\Lambda}H$, can be reconstructed via their two-body-decay channels. Their properties are of great interest as they are determined by hyperon-nucleon interactions, which are expected to be very relevant for the equation of state of highly compressed matter. Thanks to the electromagnetic calorimeter, which was used for the first time in the measurement of Ag+Ag collisions at $\sqrt{s_{NN}}$ = 2.42 and 2.55 GeV, HADES is capable of detecting photons directly. This enables the reconstruction of electromagnetic decays such as the Σ^0 hyperons [22].

Besides that, the large acceptance of the HADES experiment makes it well suited for the direct detection of strange hadrons, for example charged kaons, and thereby in a broader sense also the reconstruction of ϕ mesons via their decay into two charged kaons [23].

One of the most important observations made by HADES concerning the production of strange hadrons in Au+Au collisions at $\sqrt{s_{NN}}$ = 2.42 GeV was that independent from their

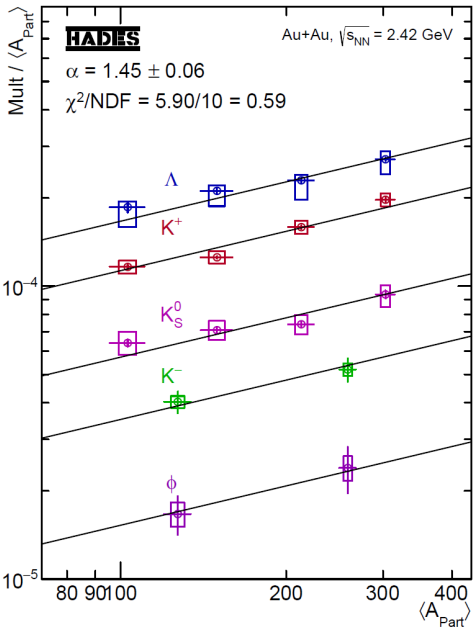

Figure 4. Production rates of Λ hyperons and K^+, K^0_S, K^- and ϕ mesons as a function of $\langle A_{Part} \rangle$ for Au+Au collisions at $\sqrt{s_{NN}}$ = 2.42 GeV (left) [24] and for Ag+Ag collisions at $\sqrt{s_{NN}}$ = 2.55 GeV (right) [20, 23]. The curves correspond to $\langle A_{Part} \rangle^{\alpha}$ functions with a global value of α shared among all hadron species.

threshold in isolated N-N collisions the production rates of all strange hadrons scale with $\langle A_{Part} \rangle$ with a similar slope as shown in figure 4 [24]. This points towards a production mechanism in which the production of strange-antistrange-quark pairs is decoupled from the distribution of these quarks to the later observed hadrons, for more details see [25]. Later this universal $\langle A_{Part} \rangle$ scaling was confirmed in Ag+Ag collisions at $\sqrt{s_{NN}}$ = 2.55 GeV [23]. Within uncertainties, the exponents determined for both collision systems (Au+Au: 1.45 ± 0.06 and Ag+Ag: 1.50 ± 0.03 [23]) are identical and do not reflect the different collision energies.

5 Summary and Outlook

On this Quark Matter conference, HADES has presented for the first time the spectra of excess radiation measured in Ag+Ag collisions at $\sqrt{s_{NN}}$ = 2.42 and 2.55 GeV as well as the extracted average fireball temperatures. Further, we presented a direct measurement of the transition form factor of the resonance-ρ coupling which supports the predictions of the vector meson dominance model. Finally, we presented measurements of the elliptic flow of di-leptons which supports the assumption that di-leptons are penetrating probes. Concerning the measurement of collective flow phenomena and two-particle correlations we presented for the first time correlations between different orders of flow coefficients enabled by the event-by-event flow measurements, where a clear dependence on the equation of state is observed in model predictions. Further, we presented two particle femtoscopy studies of proton-proton, proton-cluster, Λ-proton and γ-γ correlations [15, 16]. On the side of the study of strange hadron production, we presented the measurement of Σ^0 hyperons via direct detection of the decay γ [22] as well as the measurement of double strange Ξ^- hyperons far below their threshold in isolated N-N collisions for the first time. Finally, we put all particle measurements in context with each other by applying statistical hadronization model fits.

At the beginning of 2024, HADES is going to measure Au+Au and C+C collisions at kinetic beam energies of 0.8A GeV and below. These measurements will extend the area covered in the phase diagram of QCD matter to even higher baryochemical potentials to gain

more constraints on the equation of state of dense baryonic matter and potentially allows to discover further phase transitions. Within the next decade, the construction of the SIS100 accelerator and the CBM experiment are going to be completed and will allow us to study heavy-ion collisions in the 2.7 to 4.9 GeV energy range with unprecedented precision. The entire physics program of the CBM experiment is described in [26].

References

[1] J. Adamczewski-Musch *et al.* HADES Collaboration, Nature Phys. **15** 1040-1045 (2019).

[2] M. Hanauske, J. Steinheimer, L. Bovard, A. Mukherjee, S. Schramm *et al.*, J. Phys. Conf. Ser. **878** 012031 (2017).

[3] C. Ecker, M. Järvinen, G. Nijs and W. van der Schee, Phys. Rev. D **101** 103006 (2020).

[4] M. Creutz, *Quarks, Gluons and Lattices* (Cambridge University Press, 1984).

[5] J. Weil, V. Steinberg, J. Staudenmaier, L.G. Pang, D. Oliinychenko *et al.*, Phys.Rev.C **94** 5, 054905 (2016).

[6] S.A. Bass, M. Belkacem, M. Bleicher, M. Brandstetter, L. Bravina *et al.*, Prog.Part.Nucl.Phys. **41** 225-370 (1998).

[7] M. Bleicher, E. Zabrodin, C. Spieles, S.A. Bass, C. Ernst *et al.*, J.Phys.G **25** 1859-1896 (1999).

[8] G. Agakishiev et al. HADES Collaboration, Eur.Phys.J.A **41** 243-277 (2009).

[9] R.J: Porter et al. DLS Collaboration, Phys.Rev.Lett. 79 1229-1232 (1997).

[10] G. Agakishiev et al. HADES Collaboration, Phys. Lett. B **690** 118 (2010).

[11] R. Abou Yassine et al. HADES Collaboration, arXiv:2205.15914 [nucl-ex] (2022).

[12] R. Rapp and H. van Hees, Phys.Lett.B **753** 586-590 (2016).

[13] R. Rapp, J. Wambach and H. van Hees, Landolt-Bornstein **23** 134 (2010).

[14] P.M. Hohler and R. Rapp, Phys.Lett.B **731** 103-109 (2014).

[15] M. Grunwald *et al.* HADES Collaboration, Contribution to the present volume.

[16] M. Stefaniak *et al.* HADES Collaboration, Contribution to the present volume.

[17] S. Voloshin and Y. Zhang, Z.Phys.C **70** 665-672 (1996).

[18] J. Adamczewski-Musch *et al.* HADES Collaboration, Phys.Rev.Lett. **125** 262301 (2020).

[19] J. Adamczewski-Musch *et al.* HADES Collaboration, Eur.Phys.J.A **59** 4, 80 (2023).

[20] S. Spies, Strange Hadron Production in Ag+Ag Collisions at 1.58A GeV, PhD Thesis Goethe University Frankfurt (2022).

[21] S. Spies et al. HADES Collaboration, Acta Phys.Polon.Supp. **16** 1, 146 (2023).

[22] M. Becker *et al.* HADES Collaboration, Contribution to the present volume.

[23] M. Kohls, Production of $K^{\pm}$ and ϕ-Mesons in Ag+Ag-Collisions at 1.58A GeV, PhD Thesis Goethe University Frankfurt (2023).

[24] J. Adamczewski-Musch *et al.* HADES Collaboration, Phys.Lett.B **793** 457-463 (2019).

[25] K. Fukushima, T. Kojo and W. Weise, Phys.Rev.D **102** 9, 096017 (2020).

[26] B. Friman, C. Hohne, J. Knoll, S. Leupold, J. Randrup, R. Rapp and P. Senger, Lect.Notes Phys. **814** pp.1-980 (2011).